J Nanostruct 16(4): 5762-5771, Autumn 2026

RESEARCH PAPER

Synthesis and Characterization of NiO Nanoparticles Produced by Laser-Induced Plasma

Nada Ismael Ibrahim

Department of Physics, College of Science, University of Diyala, Diyala, Iraq

ARTICLE INFO

Article History:
Received 16 June 2026
Accepted 20 September 2026
Published 01 October 2026

Keywords:
Laser Induced Plasma
Nickel oxide
Optical Properties
Pulsed Laser Deposition
Structural Properties

ABSTRACT

In this work, NiO thin films have been synthesized by, inexpensive, pulsed laser deposition (PLD) on glass substrates with (500,600,700 and 800) mJ of laser energy, using Q-switching Nd:YAG laser. The structural, optical properties and the surface morphology of the thin films were studied and analyzed. XRD data indicated formation of a polycrystalline of face center cubic structure of NiO. Furthermore, it was proved that the structural properties were affected by the high level of laser energy, improving the films crystallinity. The absorption spectrum of prepared samples showed blue shift (change in wavelength), which is due to the reduction of particle size .The optical band gap, which is critical to the characterization of the optical properties of the films, varied between 2.7 and 3.4 eV and increased as a function of laser fluence. Surface uniformity improves as laser fluence increases, as shown in FESEM analysis. Specifically, the surface morphology of several films at 800 mJ was shown to be more homogeneous and dense. EDS analysis showed deviations from the stoichiometry of the samples, indicating that the NiO thin films may have defects related to its p-type conductivity. AFM revealed a reduction in grain size with increasing laser fluence, which may lead to greater surface-area-to-volume ratio. In these tested conditions, an energy of 800 mJ produced films with a beneficial structural and surface properties, indicating an important factor for good sensing devices.

How to cite this article
Ismael Ibrahim N. Synthesis and Characterization of NiO Nanoparticles Produced by Laser-Induced Plasma. J Nanostruct, 2026; 16(4):5762-5771. DOI: 10.22052/JNS.2026.04.105

INTRODUCTION

Laser-induced plasma (LIP) is formed through the interaction of intense laser radiation with a material when the laser irradiance exceeds a material-dependent threshold [1]. This phenomenon has attracted considerable interest because of its applications in various scientific and technological fields, including pulsed laser deposition (PLD ([2], laser ablation in liquids for nanostructure synthesis [3], and laser-induced breakdown spectroscopy (LIBS) [4], etc. Pulsed laser deposition (PLD) is a versatile technique widely employed for the in-situ fabrication of thin films and nanoscale materials. In this process, high-energy laser pulses irradiate a solid target inside a vacuum chamber, causing material ablation and the formation of a plasma plume. The ejected species subsequently travel toward a substrate, where they condense to form a thin film that may reach a thickness of several micrometers, depending on the deposition conditions [5, 6]. The window, through which a laser beam enters

* *Corresponding Author Email: nadaibrahim@uodiyala.edu.iq*

This work is licensed under the Creative Commons Attribution 4.0 International License.
To view a copy of this license, visit http://creativecommons.org/licenses/by/4.0/.

and hits the target, or the material to deposit, are located in vacuum. This results in energy of the laser-photon beam being absorbed by local solid surface, triggering electronic excitation. The thermal conductivity of the solid target is much too low to permit any significant energy dissipation during the very short duration of the laser pulse, leading to a conversion of photon into thermal and chemical energy. This results in such a high temperature (about 3500 °C) for a small volume of the target, generating instantaneous evaporation, ionization and decomposition of the material [6, 7]. The vapour consists of neutral atoms, positive and negative ions, electrons, molecules and molecular ions, free radicals of the target material in their ground state or excited states. Such correlated whirl forces picturing a mass of plasma particles is known as plume (or wavefront). These are harvested on the substrate to create a thin film [2, 7]. Rapidly-evolving and sensitive plasma processes is transient and observed to be highly dependent on incident laser fluence (laser energy/pulse area), wavelength, ambient gas composition, and pressure [6]. Nanocrystalline metal oxides have received increasing attention because of their potential applications in various fields. Among these materials, nickel oxide (NiO) is a p-type semiconductor characterized by good chemical stability and a wide band gap of approximately 3.6–4.0 eV [8-10]. These properties make NiO a potential candidate for applications in solar cells, catalysis, sensors, and optoelectronic devices [10-12]. NiO thin films have been prepared by various techniques such as sol–gel [13], co-precipitation [14], spray pyrolysis technique (SPT) [15], Dc magnetron sputtering [16], microwave method (MM) [17], electron beam evaporation techniques [18], chemical vapour deposition (CVD) [19], and atomic layer deposition (ALD) [20]. PLD is a versatile process. It can accurately control the composition, structure and growth rate of the film. It is an important technology for preparing high-quality thin films and is well suited to regulate the properties of the film [6, 21]. In this study, the structural, optical and morphological properties of NiO thin films prepared by PLD method were investigated.

MATERIALS AND METHODS

The PLD was performed in a vacuum chamber of 2.5×10^{-2} mbar pressure. A Q-switched Nd:YAG laser beam was passed through a Pyrex glass window at an incidence angle of 45° to the target surface normal. The substrate was placed opposite the target surface, separated 2 cm from it. It also prevented the substrate holder from interfering with the path of the incoming laser beam. The films were deposited over 200 laser pulses using a Q-switched Nd:YAG laser at λ = 1064 nm (1.16 eV) with pulse energies of either 500,600,700, or 800 mJ. The target was periodically rotated around its axis to reveal a new surface, mitigating the effects of irradiating the same spot multiple times. This focused laser beam ablated a small amount of target material, which has been transported into the substrate and deposited on glass surfaces (Fig. 1).

High-purity nickel oxide (NiO) powder (99.99%) was used to prepare the targets for thin-film deposition. A total of 2 g of powder was compressed into pellets using a hydraulic press. The resulting pellets had a diameter of 10 mm and a thickness of 4 mm. These pressed pellets were used as target materials for the deposition process.

X-ray diffraction (XRD) measurements were performed at room temperature using Cu Kα radiation with a wavelength of 1.5406 Å. The operating voltage and current were set to 40 kV and 30 mA, respectively. The scanning speed was 5°/min. Based on Scherrer equation, average crystallite size (D) for the sample were calculated as follow [22, 23]:

$$D=(k\lambda)/\beta\ COS\theta \quad (1)$$

In Scherrer equation, λ, β, and θ are the X-ray wavelength, full width at half maximum (FWHM) of the diffraction peak and Bragg diffraction angle, respectively. The surface morphology and microstructure of the NiO thin films were performed on glass substrates using an Inspect S50 SEM. In addition, atomic force microscopy (AFM) of the NiO thin films was employed to further investigate the surface topography and distribution of features across the samples using a CSPM-5000 scanning probe microscope.

RESULTS AND DISCUSSION

XRD analysis

The XRD patterns for NiO films obtained using varying amounts of laser energy are shown in Fig. 2. It was found that all samples revealed a polycrystalline. The five most intense diffraction

(cc) BY

peaks centered at 2θ= 37.24°, 43.32°, 62.88°,75.29° and 79.28° which indexed to the planes of (111), (200), (220), (311) and (222), respectively, matched with JCPDS card No. 47-1049 of face center cubic structure of NiO [24]. No additional diffraction peaks arising from secondary crystalline phases observed for NiO films, indicating that all prepared thin films of these samples were pure. With increasing laser pulse energy, slight shifts in peak positions may be related to effects of lattice strain and crystallite size's changes. The XRD patterns revealed that the peak intensity increases and the peak width decreases with increasing laser pulse energy, suggesting an enhancement in crystallinity and crystallite size (Table 1). Higher particle sizes with laser energy (of more laser energy) are enable

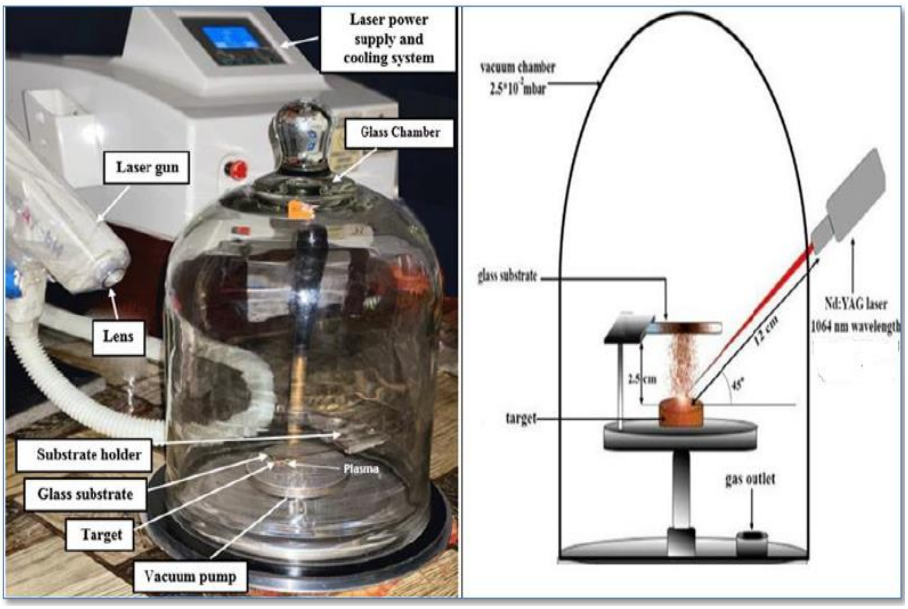


Fig. 1. The schematic of PLD method using Nd: YAG with λ=1064 nm.

Table 1. Variation in the XRD parameters of NiO thin films with laser pulse energy.

Laser Energy (mJ)	2θ (Deg.)	FWHM (Deg.)	d_{hkl} (Å)	D (nm)	Average crystalline size	hkl
	36.9886	0.7510	2.4284	11.2		(111)
500	43.0329	0.7868	2.1002	10.9	11.1	(200)
	62.6323	0.8226	1.4820	11.3		(220)
	37.1316	0.7153	2.4193	11.7		(111)
600	43.1402	0.7511	2.0953	11.4	11.7	(200)
	62.7396	0.7800	1.4798	11.9		(220)
	37.2370	0.6937	2.4127	12.1		(111)
700	43.2117	0.7010	2.0920	12.2	12.3	(200)
	62.8112	0.7300	1.4782	12.8		(220)
	37.2389	0.6438	2.4126	13.0		(111)
800	43.3190	0.6796	2.0870	12.6	12.9	(200)
	62.8827	0.7110	1.4767	13.1		(220)

CC BY

to the ablation of larger quantities of the target and also, the higher energy aids to amalgamate small particles between them [25].

Optical properties

The optical absorption spectra of NiO nanostructures prepared at laser pulse energies ranging from 500 to 800 mJ are shown in Fig. 3. The range of the spectra is 300–1100 nm. The absorption peaks at 352, 333, 322 and 311 nm corresponding to the pulse energies of 500,600,700 and 800 mJ, respectively, was associated with the effect of quantum confinement of the nanostructure on carrier generation (electron - hole) [26]. As the laser pulse energy increased, the absorption peak shifted toward shorter wavelengths, indicating a blue shift that may be associated with changes in particle size, as suggested by the SEM and AFM observations [27]. The absorption spectra also showed differences in the visible and near-infrared regions. These variations may reflect changes in the optical properties and morphology of the prepared NiO nanostructures. However, the shift cannot be attributed solely to particle-size reduction. The relationship between wavelength and absorbance depends on the material's optical properties and the interaction of light with the film [9]. In such a case, absorbance factor increases. The absorption spectra showed an enhancement in absorption intensity and peak broadening as the laser pulse energy increased. These changes may be associated with variations in the size and structural properties of the NiO nanoparticles, as reported in a previous study [28]. In contrast, the transmittance spectra exhibited an opposite trend, as shown in Fig. 4.

The optical band gap energy (Eg) is an important parameter for characterizing semiconductor materials and determining their potential for optical and electronic applications. It is thereby related to material structural and electronic properties, which are determined by the arrangement of the atoms in a crystal lattice. The value of Eg is dictated by the crystal structure, indicating that it responds to local atomic arrangement in semiconductors [29, 30]. The value of band gap energy for NiO films was estimated by using Tauc equation [22]:

$$\alpha h\nu = C\,[(h\nu - Eg)]^{n} \qquad (2)$$

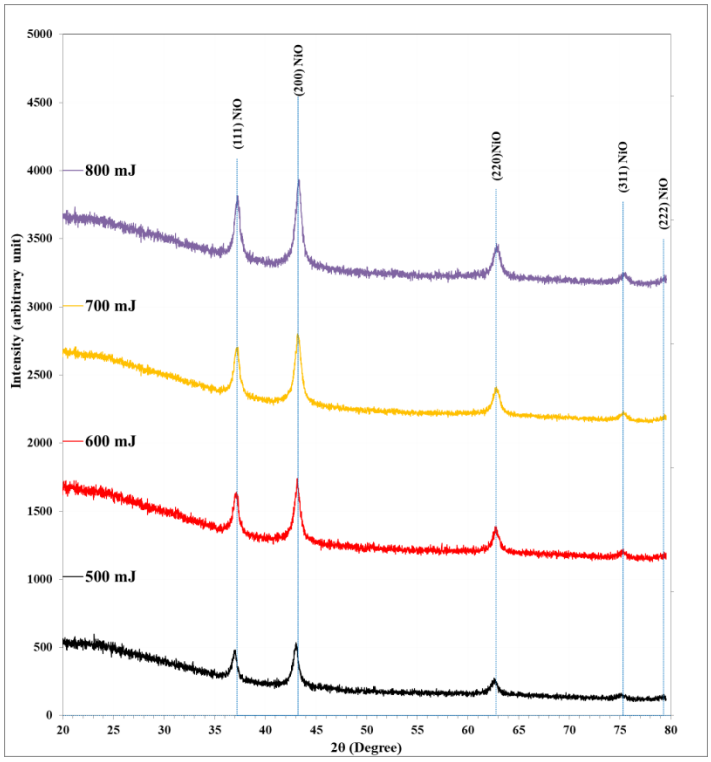


Fig. 2. XRD patterns of prepared NiO nanostructure in 500-800 mJ.

CC BY

In this equation, α represents the absorption coefficient, hν denotes the photon energy, and C is a proportionality constant. The exponent n depends on the type of electronic transition, n =1/2 for a direct allowed transition and n = 2 for an indirect allowed transition [31]. Fig. 5 shows the variation of $[(\alpha h\nu)]^2$ as a function of incident photon energy (hν). Values of the band gab energy have been extracted from an extrapolation of the linear region for the curve to intersect with the energy axis (hν). The estimated optical band gap values were 2.7, 3.0, 3.1, and 3.4 eV for NiO films prepared at laser pulse energies of 500, 600, 700, and 800 mJ, respectively. The enhancement in band gap may be associated with changes in particle size and the resulting quantum confinement effects, although this interpretation requires supporting evidence of nanoscale dimensions [28]. Furthermore, it is noted that the Eg values obtained for NiO thin films in this work indicated that performance has positively related to film crystallinity, which also verifies with earlier experiments [26, 31].

Morphology

The FESEM images of NiO nanostructures

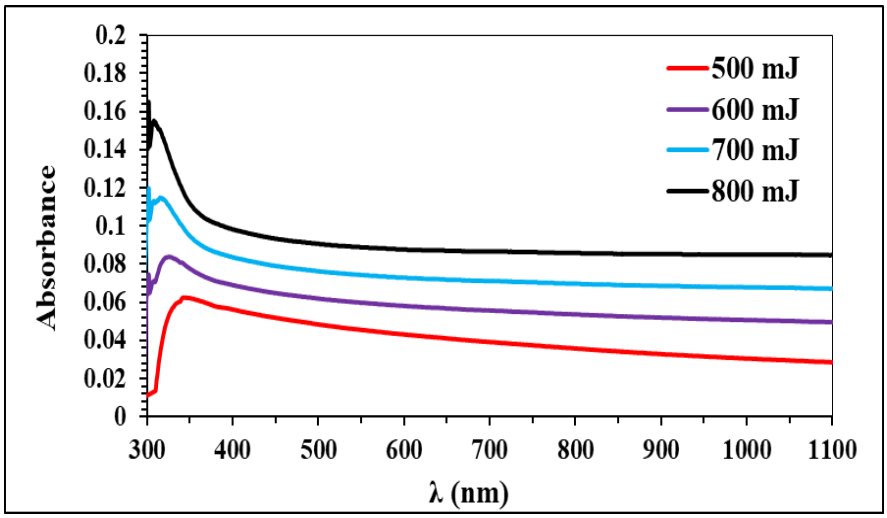


Fig. 3. Absorbance spectra of NiO nanoparticles as a function of wavelength at different laser energies.

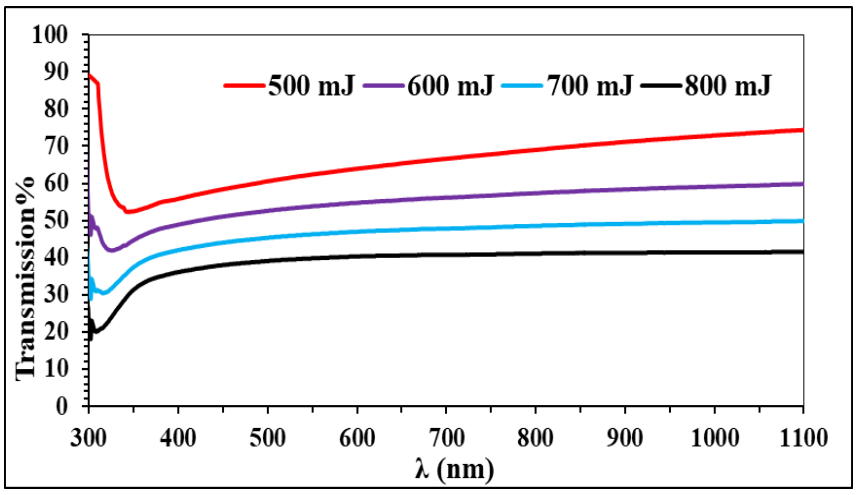


Fig. 4. Transmission spectra of NiO nanoparticles at different laser energies.

CC BY

prepared at different laser energies are indicated in Fig. 6. This Figure clarified that at a lower value of laser fluence (500 mJ), the apparent grain size is relatively large due to the coalescence and clustering of smaller particles, a phenomenon known as agglomeration, where the emergence of agglomeration in thin films is associated with PLD [32]. As illustrated in Fig. 6b, and Fig. 6c, the thin films have low agglomeration, as energy increases. Whereas, at the highest value of laser fluence (800

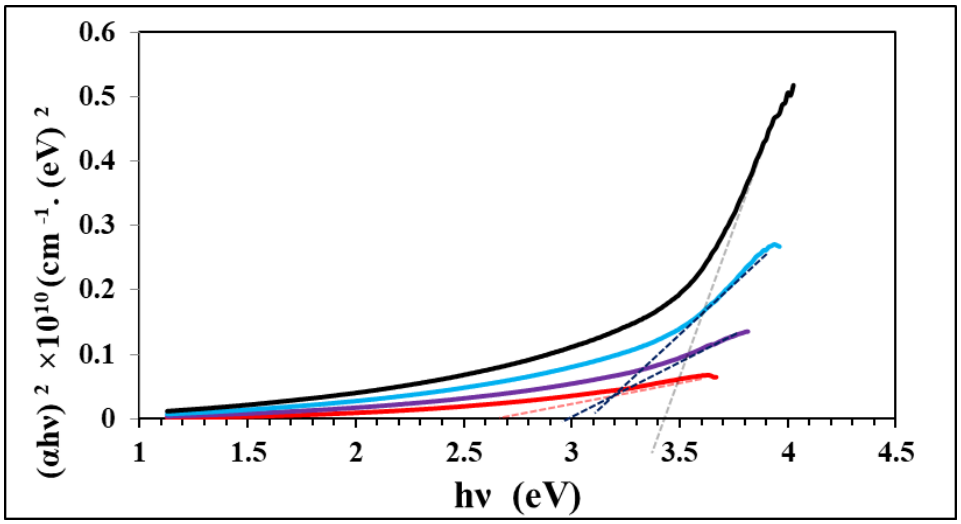


Fig. 5. Tauc curves of the synthesized NiO nanostructure at various laser energies.

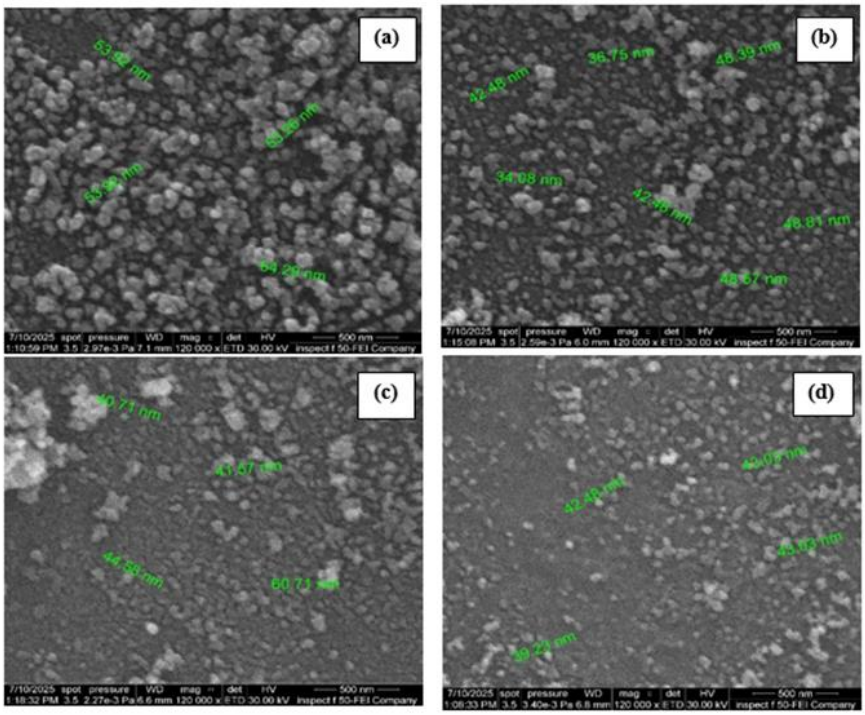


Fig. 6. FE-SEM images of NiO nanoparticles at: (a) 500 mJ, (b) 600 mJ, (c) 700 mJ, and (d) 800 mJ.

(cc) BY

mJ), film surface appears more homogeneous and dense. It geographies a widespread, dense distribution of nano-sized grains. Therefore, as the laser energy increases during PLD process, the produced amount of materials increases and the particle size decreases. Variations in particle size can be explained by the balance between nucleation and growth processes occurring at lower or higher laser energy levels, respectively. When the laser energy is low, fewer nuclei form that allow for the available material to help in forming larger particles. Higher laser energies may favor formation of more nuclei and hence smaller particles. The particle size can be affected by many factors like ablation rate, transport of material and growth conditions [33, 34]. This morphology is anticipated to increase the effective surface area and improve the sensing performance of the NiO film.

EDS analysis

EDS is a general analytical method for the detection and quantitative measurement of any element in trace amounts within a material. The electron beam interacts with the sample and this interaction almost releases the X-ray characteristics. The energies of theses X-rays are used to identify the elements, and their intensities provide information on the elemental composition. Fig. 7(a-d) presents the EDS spectra for the NiO nanoparticles, revealing the presence of peaks corresponding to nickel (Ni) and oxygen (O) at laser pulse energies ranging from 500 to 800 mJ, respectively. EDS analysis provided information on the elemental composition of the synthesized NiO nanoparticles, complementing the structural data obtained *via* XRD. As shown in Fig. 7, the spectra exhibit characteristic signals for nickel (Ni) and oxygen (O), with their respective weight and atomic percentages provided for each sample. The horizontal axis represents X-ray energy (in keV), while the vertical axis indicates the number of detected X-ray pulses. The measured Ni-to-O ratios deviate from the ideal stoichiometric composition, suggesting a non-stoichiometric structure. These deviations may be linked to defects within the NiO lattice and are consistent with its behavior as a p-type semiconductor. However, EDS analysis is insufficient to definitively identify the specific type of defects or to reveal the origin of the p-type electrical conductivity [35].

AFM analysis

AFM was study the characterize NiO's surface topography obtained by PLD at 500–800 mJ of laser energy. As shown in Fig. 8, at the lower value of laser fluence (500 mJ), the image consists of large agglomerations with smooth upper surfaces.

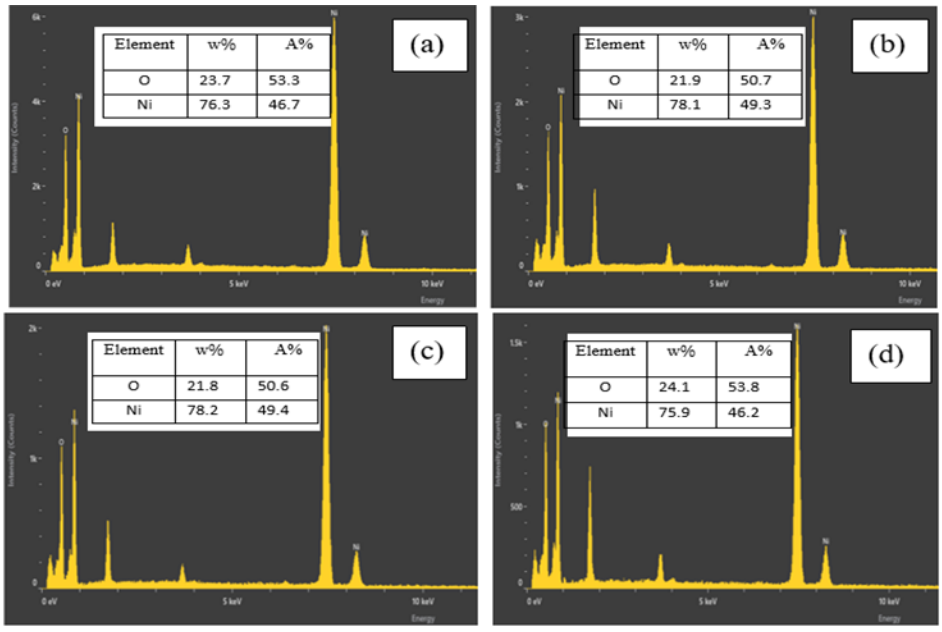


Fig. 7. EDS spectra of NiO nanoparticles at: (a) 500 mJ, (b) 600 mJ, (c) 700 mJ, and (d) 800 mJ.

CC BY

This is agreement with FESEM image. These large clusters reduce the specific surface area and leads to an inhomogeneous grain distribution across the film surface [36]. Contrary, at the highest value of laser fluence (800 mJ), image clearly exhibits highly dense, closely packed nanostructures. This massive number of micro-peaks and valleys indicates a significant enhancement in the number of grains per unit area, accompanied by a reduction to the nanoscale. However, as the energy increases, the grain size tends to decrease, resulting in the formation of smaller crystalline grains [37]. Consequently, this leads to a higher surface area compared to the agglomerated NiO-500 sample, even though the roughness of the current sample is higher than that of the NiO-800 sample. Where, the average roughness may decrease with increasing laser pulse energy due to changes in surface morphology, such as improved surface uniformity or grain refinement [37]. Similarly, the root mean square roughness, which reflects variations in surface height, may also decrease under certain deposition conditions. These trends depend on the material and the laser parameters used [38]. Table 2 includes AFM parameters such as average roughness, mean diameter, and root mean square height deviation. The results showed that the sample prepared at 800 mJ have the highest quality, which is an important factor for gas sensing applications.

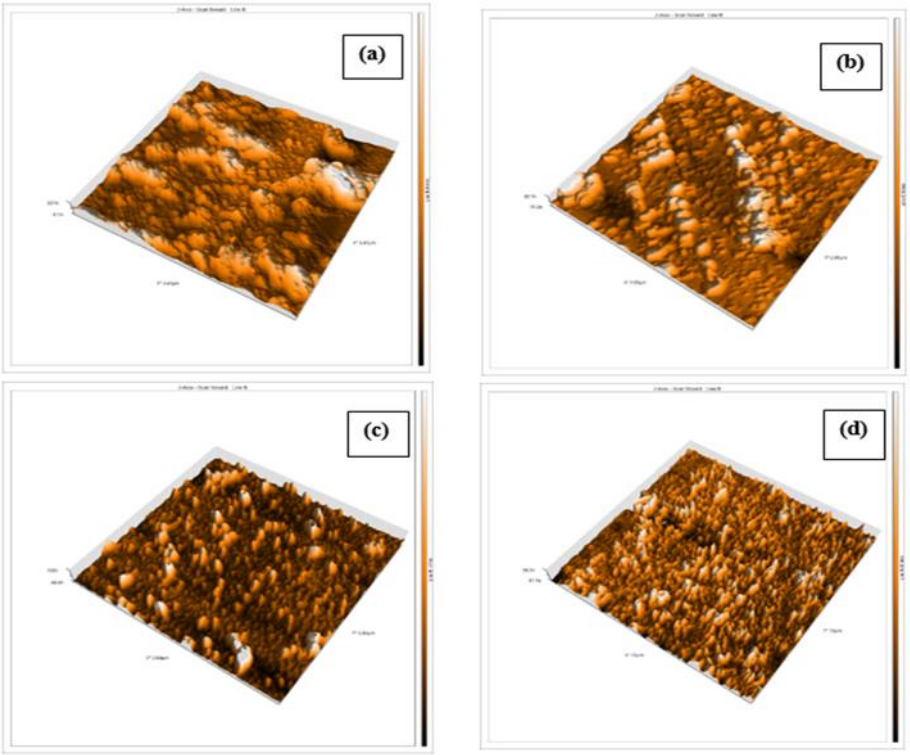


Fig. 8. 3D AFM for NiO prepared at: (a) 500 mJ, (b) 600 mJ, (c) 700 mJ, and (d) 800 mJ.

Table 2. AFM parameters of NiO thin films prepared at different laser pulse energies.

Laser energy(mJ)	Roughness (nm)	Average diameter (nm)	Root mean square height (nm)
500	110.7	142.1	136.2
600	79.73	46.44	94.57
700	47.87	90.84	58.55
800	101.7	80.37	117.4

CC BY

CONCLUSION

NiO thin films were deposited by PLD on glass substrates at different laser energy (500, 600, 700, and 800 mJ), and then examined. Results from XRD revealed that NiO films consists a polycrystalline face center cubic structure and the degree of crystal growth of the films was raised with increasing laser energy. In addition, optical investigation was demonstrated that nanoscale electron confinement (quantum size effect) led to an enhancement in the NiO thin film's energy gap with decreasing sizes. The FESEM results illustrated more homogeneous and dense films surface of NiO grown at 800 mJ, while the EDS results revealed non-stoichiometric behavior of p-type NiO semiconductor. Similarly, AFM results exhibited minimum grain size and maximum surface area at 800 mJ. Therefore, the optimized NiO thin films with 800 mJ was found to be the best for gas sensors applications.

CONFLICT OF INTEREST

The authors declare that there is no conflict of interests regarding the publication of this manuscript.

REFERENCES

1. De Giacomo A, Hermann J. Laser-induced plasma emission: from atomic to molecular spectra. Journal of Physics D: Applied Physics. 2017;50(18):183002.
2. Ahmed RT, Ahmed AF. Influence of Laser Energy on the Structural and Optical Properties of Sn Nanoparticles produced with Laser-Induced Plasma. Iraqi Journal of Physics. 2024;22(2):69-80.
3. Jassim NM, Ibrahim NI. Z-Scan Study of the Non-linear Optical Properties of Silver/Curcumin Dye Nanocomposites Prepared Via Nanosecond Pulsed Laser Ablation. Revue des composites et des matériaux avancés. 2024;34(4):533-540.
4. Abbas AK, Aadim KA, Jawaad MF. Spectroscopic diagnostic of (Zn:NiO) plasma by laser induced breakdown spectroscopy. AIP Conference Proceedings: AIP Publishing; 2021. p. 080013.
5. Mahdi RO, Hadi AA, Taha JM, Khashan KS. Preparation of nickel oxide nanoparticles prepared by laser ablation in water. AIP Conference Proceedings: AIP Publishing; 2020. p. 020309.
6. Haider AJ, Alawsi T, Haider MJ, Taha BA, Marhoon HA. A comprehensive review on pulsed laser deposition technique to effective nanostructure production: trends and challenges. Optical and Quantum Electronics. 2022;54(8).
7. Hegde MS. Epitaxial oxide thin films by pulsed laser deposition: Retrospect and prospect. Journal of Chemical Sciences. 2001;113(5-6):445-458.
8. Allali M, Dahamni MA, Ghamnia M, Boukhachem A, Boukrédimi D, Tonneau D, et al. Synthesis and Investigation of Pure and Cu-Doped NiO Nanofilms for Future Applications in Wastewater Treatment Rejected by Textile Industry. Catalysts. 2022;12(9):931.
9. Hussain N, Abbas L, Latif L. Preparation of Nickel Oxide Microparticles by Pulsed Laser Ablation and Application to Gas Sensors. Engineering and Technology Journal. 2021;39(6):1011-1018.
10. Dikovska A, Avdeev G, Atanasova G, Dilova T, Nikov R, Nedyalkov N. ZnO-NiO composite nanostructures produced by atmospheric PLD. Journal of Physics: Conference Series. 2023;2487(1):012002.
11. Hu Z, Chen D, Yang P, Yang L, Qin L, Huang Y, et al. Sol-gel-processed yttrium-doped NiO as hole transport layer in inverted perovskite solar cells for enhanced performance. Applied Surface Science. 2018;441:258-264.
12. Harb NH. Preparation and characterization of NiONPS sensor Prepared by Different Q-switched Nd: YAG Laser parameter: energy pulse and wavelength. Baghdad Science Journal. 2024.
13. Hasson SS, Alsammarraie AMA. Synthesis of nickel oxide nanoparticles by Sol-gel method. International journal of health sciences. 2022:48938-48947.
14. Atul AK, Srivastava SK, Gupta AK, Srivastava N. Synthesis and Characterization of NiO Nanoparticles by Chemical Co-precipitation Method: an Easy and Cost-Effective Approach. Brazilian Journal of Physics. 2021;52(1).
15. Das L, Canto-Aguilar EJ, Tapani T, Lin H, Bhuvanendran H, Boulanger N, et al. NiO thin films fabricated using spray-pyrolysis technique: structural and optical characterization and ultrafast charge dynamics studies. Journal of Physics D: Applied Physics. 2024;57(38):385303.
16. Salunkhe P, A V MA, Kekuda D. Investigation on tailoring physical properties of Nickel Oxide thin films grown by dc magnetron sputtering. Materials Research Express. 2020;7(1):016427.
17. Azhagu Raj R, AlSalhi M, Devanesan S. Microwave-Assisted Synthesis of Nickel Oxide Nanoparticles Using Coriandrum sativum Leaf Extract and Their Structural-Magnetic Catalytic Properties. Materials. 2017;10(5):460.
18. Guo X, Wang W, Wen R-T. Enhanced Electrochromic Performance by Anodic Polarization in Nickel Oxide Films. Crystals. 2021;11(6):615.
19. Wilson RL, Macdonald TJ, Lin C-T, Xu S, Taylor A, Knapp CE, et al. Chemical vapour deposition (CVD) of nickel oxide using the novel nickel dialkylaminoalkoxide precursor [Ni(dmamp')$_2$] (dmamp' = 2-dimethylamino-2-methyl-1-propanolate). RSC Advances. 2021;11(36):22199-22205.
20. Koshtyal Y, Nazarov D, Ezhov I, Mitrofanov I, Kim A, Rymyantsev A, et al. Atomic Layer Deposition of NiO to Produce Active Material for Thin-Film Lithium-Ion Batteries. Coatings. 2019;9(5):301.
21. Cai J, Li F, Zhang X, Wang J, Yu Z, Feng B, et al. Application of Pulsed Laser Deposition (PLD) Technology in the Preparation of Two-Dimensional (2D) Film Materials. Materials. 2025;18(13):2999.
22. Hammoodi FG, Mohammed FY, Ibrahim NI, Khodair ZT. Synthesis and characterization of (Fe2O3:Al) nanostructures thin films. Journal of Optoelectronic and Biomedical Materials. 2025;17(4):291-302.
23. Yaseen A, Khodair ZT, Jassim NM. Development of In2O3–WO3/porous silicon PN junctions by PLD for enhanced photodetector performance. Journal of Materials Science: Materials in Electronics. 2026;37(7).
24. Tan G, Tang D, Wang X, He L, Mu T, Li G. Preparation of NiO Thin Films and Their Application for NO2 Gas

CC BY

Detection. International Journal of Electrochemical Science. 2022;17(5):220551.
25. Bhattacharya D. Plasma dynamics from laser ablated solid lithium. Pramana. 2000;55(5-6):823-833.
26. Mostafa AM, Mwafy EA. The effect of laser fluence for enhancing the antibacterial activity of NiO nanoparticles by pulsed laser ablation in liquid media. Environmental Nanotechnology, Monitoring and Management. 2020;14:100382.
27. Ghougali M, Belahssen O, Chala A. Structural, Optical and Electrical Properties of NiO Nanostructure Thin Film. Journal of Nano- and Electronic Physics. 2016;8(4(2)):04059-04051-04059-04054.
28. Ghdhaib BM, Rashid SN. Characterization of Nickel Oxide Nanoparticles Prepared Via Pulsed Laser Ablation: Evaluated the Influence of Laser Parameters. Journal of University of Anbar for Pure Science. 2024;18(2):203-212.
29. Wang XH, Li RB, Fan DH. Study on synthesis and optical properties of Al-doped ZnO hierarchical nanostructures. AIP Advances. 2011;1(1).
30. Zheng BJ, Lian JS, Zhao L, Jiang Q. Optical and electrical properties of Sn-doped CdO thin films obtained by pulse laser deposition. Vacuum. 2011;85(9):861-865.
31. Chen G-J, Lin C-M, Shih Y-H, Jian S-R. The Microstructures and Characteristics of NiO Films: Effects of Substrate Temperature. Micromachines. 2022;13(11):1940.
32. Pershukov I. Innovative piezoelectric materials elaborated by Pulsed Laser Deposition (PLD): Agence Bibliographique de l'Enseignement Supérieur.
33. Polit O, Pastukhov AI, Kabashin AV, Itina TE, Sadegh Shakeri M, Dziedzic A, et al. Femtosecond Laser Ablation-Based Interfacial Engineering of Magneto-Plasmonic Janus Au–Ni and Au–Co Nanoparticles for Multifunctional Applications. ACS Applied Nano Materials. 2026;9(24):11269-11282.
34. Vilas AM, Boutinguiza M, Arias, Mónica F. Introduction to Laser Ablation Synthesis of Nanoparticle Solutions. Laser Based Manufacturing: CRC Press; 2026. p. 315-350. http://dx.doi.org/10.1201/9781003799023-15
35. Taeño M, Maestre D, Cremades A. An approach to emerging optical and optoelectronic applications based on NiO micro- and nanostructures. Nanophotonics. 2021;10(7):1785-1799.
36. M. Aziz D, M. Mamand D, Hassan SA, Mohammed PA, Aziz SB, Hassan HS, et al. Thermally tuned green-synthesized NiO nanostructures exhibiting enhanced crystallinity, band gap narrowing, and superior photocatalytic activity toward organic dye degradation. RSC Advances. 2026;16(44):55680-55702.
37. Gupta V, Sreenivas K. Pulsed Laser Deposition of Zinc Oxide (ZnO). Zinc Oxide Bulk, Thin Films and Nanostructures: Elsevier; 2006. p. 85-174. http://dx.doi.org/10.1016/b978-008044722-3/50004-x
38. Suad MK. Characterization of Nanocrystalline SnS Thin Film Fabricated used PLD Method for Photodetection Applications. International Journal of Nanoelectronics and Materials (IJNeaM). 2024;17(2):172-179.

CC BY